Proceedings of Eurodrying'2019
Torino, Italy, July 10-12, 2019

Paper 073

STATIONARY AND TRANSIENT ASPECTS OF AIR FLOW IN A NOVEL RADIAL MULTI-ZONE DRYER

U. Jamil Ur Rahman[1], A.K. Pozarlik[1], I. Baiazitov[1], T. Tourneur[2], A. de Broqueville[2], J. De Wilde[2], G. Brem[1]

[1]Thermal Engineering, Department of Thermal and Fluid Engineering, University of Twente
5, Drienerlolaan, 7522 NB Enschede
Email: u.jamilurrahman@utwente.nl
[2]Materials & Process Engineering Division, Université Catholique de Louvain
IMAP, Place Sainte Barbe 2/L5.02.02, 1348 Louvain-la-Neuve

Abstract
In order to develop a commercially viable alternative spray drying technology, a high drying rate in a small volume must be achieved whilst maintaining a small residence time. This can be accomplished in a radial multizone dryer where high air inlet temperatures and high-G fluidization leads to enhanced drying rates. In this paper, results of CFD model are presented and validated against experimental data. The results show radial oscillations of central hot air flow with a frequency of 3.5 Hz.

Keywords*: spray dryer, vortex chamber(s), process intensification, CFD, transient*

1. Introduction

Spray drying is a highly energy intensive unit operation that has long suffered from high investment and operating costs. The process is widely used for production of powders from liquid feeds (Masters, 1985). In this work, a process intensified spray drying technology is presented, known as Radial Multizone Dryer (RMD) which is a variant of vortex chamber (Broqueville, A. de et al., 2018; De Wilde & de Broqueville, 2008) with an addition of cylindrical extension wherein a free vortex is generated i.e. without tangential air inlets thus, reducing the required air flow consumption.

In a RMD, two distinct temperature zones exists: a central hot zone (350 °C) where droplets are sprayed counter-current with the hot air and spend a very short residence time (milliseconds) followed by rapid evacuation of dried particles -by the strong centrifugal forces- to the mild temperature rotating zone (100 °C) thus, avoiding product degradation. In this cold peripheral rotating zone, high-G acceleration further enhances the interfacial heat, mass and momentum exchange as well as effective separation of particles from air (De Wilde, 2014; Weber et al., 2017).

The previous experimental and computational studies (Rahman et al., 2018; Tourneur et al., 2018) on multi-zone vortex chamber concept have revealed the presence of two distinct temperature zones, efficient spray-air contact and high evaporation rates. However, in order to successfully realize the counter-current spray drying process, protection of the spray nozzle from milk deposition is necessary to avoid clogging and overheating of the nozzle tip and walls. This has led to a new sleeve design for nozzle protection with additional co-flows around the nozzle with the spray.

The high temperatures and multiphase flow in spray drying makes it difficult to run experiments and optimize the dryer. Computational Fluid Dynamics (CFD) modeling has been widely recognized in understanding the complex multiphase and transient nature of flow fields inside spray dryers (Kieviet, 1997; Kuriakose & Anandharamakrishnan, 2010; Langrish & Fletcher, 2003; Saleh & Nahi Saleh, 2011). In this paper, an experimentally validated CFD model is developed for air flow only which is then used to investigate the unsteady characteristics of air flow in RMD by which the frequency of oscillations can be recognized. The focus of this paper is on the interaction of the hot air and counter-current nozzle flows and therefore, only air flow is simulated i.e. without inclusion of spray injection.

2. Material and method

The geometry of RMD simulated in this study is shown in Fig.1. along with the boundaries depicting inlets and outlets of the dryer. In this setup, two temperature zones exist: a central hot zone and a high-G peripheral rotating cold zone. The droplets can be sprayed in counter-current with hot air or a combination of counter and co-current (hot co-flow) as shown in Fig.1.

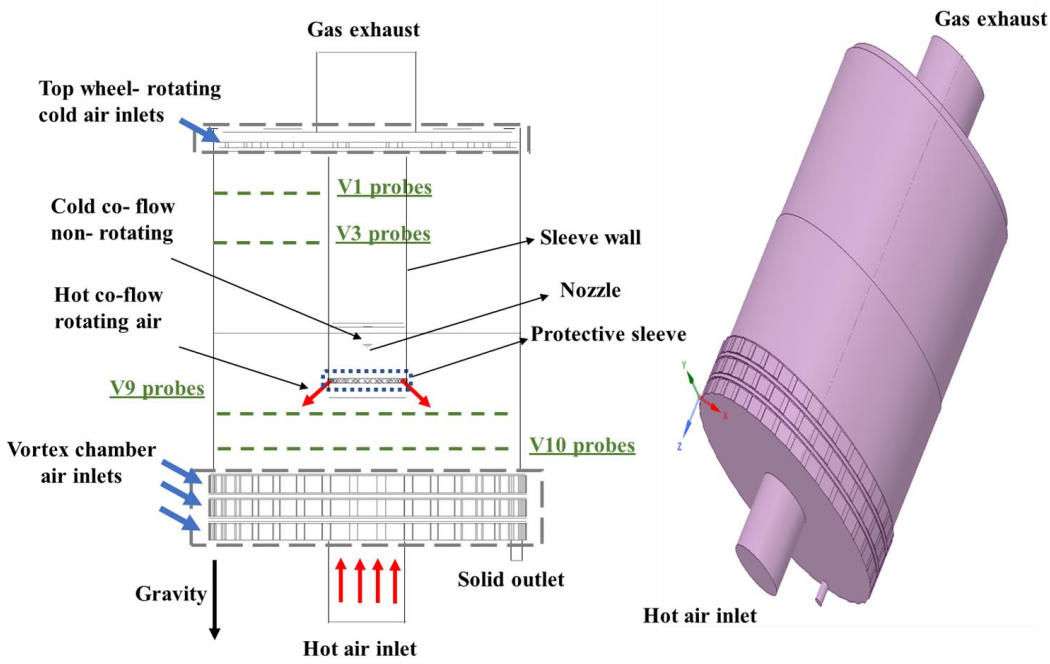

Figure 1 Geometry of RMD used in the simulations, left: schematic of RMD dryer right: 3d model of the geometry used in simulation

The spray nozzle is surrounded with a protective sleeve to avoid droplets refluxes on to the nozzle and hence, avoiding milk burning on the nozzle tip that leads to clogging and instable spray. The rotating co-flow moves the droplets outwards to the periphery while a small amount of cold flow is used to avoid overheating of the nozzle walls. In this study, however, only the gas flows are simulated i.e. the instabilities arising from the interaction of the two counter air flows. Hot air enters the dryer through a honey comb flow distributor hence, reducing small turbulences in the cylinder. The Vortex Chamber (VC) consists of 3 wheels, each wheel consisting of 36 inlet slots through which air enters the chamber tangentially, creating a high-G vortex. Further, an additional single wheel with 16 tangential inlets is used to introduce a rotating flow that separates the fine particles from

Table 1 Boundary conditions used in the simulation

Boundary settings	values
Hot air mass flow rate (kg/hr)	500
Hot air temperature (°C)	346
VC air mass flow rate (kg/hr)	305
VC air temperature (°C)	141
Top wheel air mass flow rate (kg/hr)	275
Top wheel inlet air temperature (°C)	108
Hot co-flow rotating air mass flow rate (kg/hr)	196
Hot co-flow rotating air temperature (°C)	192
Cold non-rotating air mass flow rate (kg/hr)	72
Cold non-rotating air temperature (°C)	40
Chamber thickness (m)	0,004
Air temperature outside wall (°C)	20
Pressure at outlet (Pa)	-8000

exhaust air. This rotating vortex further moves the particles axially downwards to the Vortex Chamber (VC) for final drying and removal via solid outlet. The boundary settings used in the simulation are given in Table 1. The heat losses of the cylinder walls are taken into account while no heat losses are considered for VC since, these are surrounded with air distribution jackets.

For computations, an unstructured tetrahedral mesh of 11M elements was used. The simulations have been performed in the commercial CFD package FLUENT 14.5. A 3D steady-state and transient computation with k-omega SST turbulence model was used to simulate the gas flow. All the transport equations were discretized in space using second order upwind scheme. The transient simulation was carried out using steady state solution as the initial condition. A time step of 0,001s was adopted. Typically 10-30 iterations led to a convergent solution at each time step with local residuals of less than 10^{-4}- 10^{-6}. The SIMPLE pressure-velocity coupling scheme was used. The details of the CFD methodology and the governing Navier-Stokes and turbulence model equations can be found in the literature and FLUENT user guide (ANSYS, 2004; Fletcher, 2017; Wai Woo et al., 2009).

3. Results and discussion

This section presents the predicted steady-state and transient results of the CFD model. The results are validated against the available experimental data. Further, the steady-state results re compared with the transient results.

3.1. Steady-state results

The Figure 2a shows the comparison of predicted steady-state results with the experimental measurements for probe locations V1 and V3 (see also Fig.1.). The model makes a good agreement with an average error of 2.7% for both probes: V1 and V3. It can be seen that model slightly overpredicts the temperature near the walls. The error can be caused since, the heat losses in the experimental setup are not exactly known. It can be seen that the temperature increases from the wall of the dryer towards the sleeve. Figure 2b shows the comparison of the steady-state results with the experimental data for thermocouples: V9 and V10. The model shows a similar trend with an over estimation of temperature with an average error of 7.5% and 9.5% for probes V9 and V10, respectively. The bigger error at these locations is due to intense mixing of the hot air jet, rotating hot co-flow and non-rotating cold flow. The errors arise due to the central hot air jet oscillations in the radial direction induced by the interaction of central hot air and the rotating hot air in the opposite direction. Further, it should be noted that the valley in the numerical data (central region) as presented in Fig.2b has its origin in not well premixed cold air, whereas during experiments air could be premixed and due to nozzle and sleeve contact, heated up already earlier.

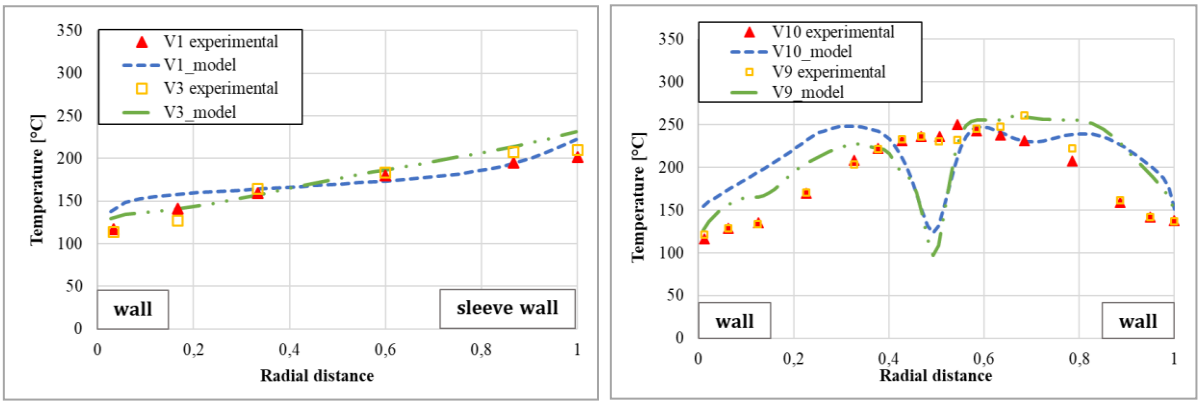

Figure 2 CFD model validation with experimental data a) V1 and V3 (left), b) V9 and V10 (right)

3.2. Comparison of transient and steady-state results

The Figure 3a presents the predicted transient profile on V10 probe (fifth location from the wall at probe V10 is selected for analysis) compared with the steady-state model result and time averaged experimental measurement. The plot indicates the oscillations of the hot air jet approximately between 190-280 °C, and thus the time dependent nature of the flow. The overprediction of the steady-state model results as seen in Fig. 2a and 2b may arise from the unstable behaviour of the hot air jet. This

in-stationary phenomena of the hot air jet is also evident from Figure 3b, where the predicted transient profiles on V10 probe is plotted at three different time steps: 0.5s, 1s and 1.5s compared with the steady-state profile and time averaged experimental measurements. It depicts the oscillatory behaviour of the flow field. The frequency of oscillations is found to be 3.5 Hz.

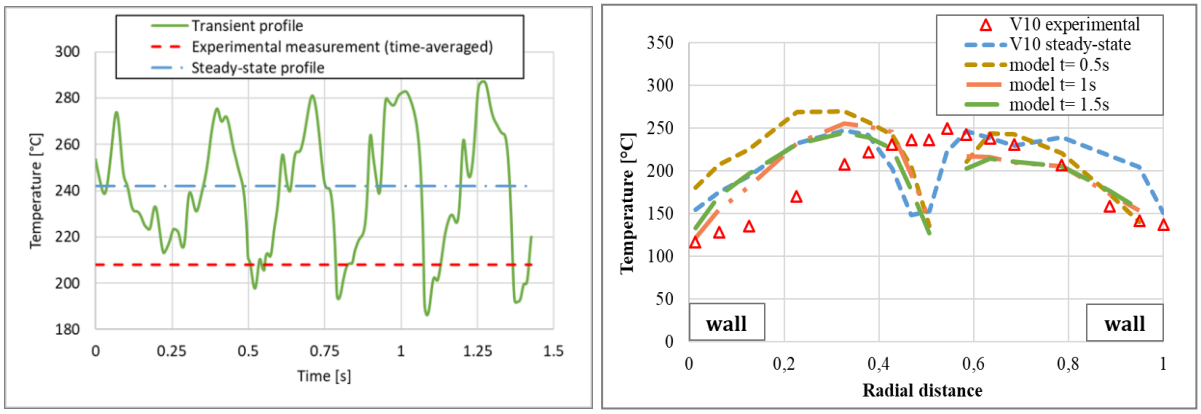

Figure 3 Comparison of transient and steady-state profiles a) at V10-5 (left), b) location V10 (right)

3.3. Comparison of temperature patterns

In this section, in order to understand the origin of instabilities of hot air jet, a sensitivity analysis is conducted. The Figure 4 compares the temperature fields for three cases: a) the reference case as presented in Table 1 b) without the co-flows around the nozzle and c) without the non-rotating cold flow around the nozzle.

In case a) (the reference case), when both: rotating and non-rotating co-flows around the nozzle are applied, the hot air jet oscillates radially giving asymmetrical temperature patterns. Due to the in

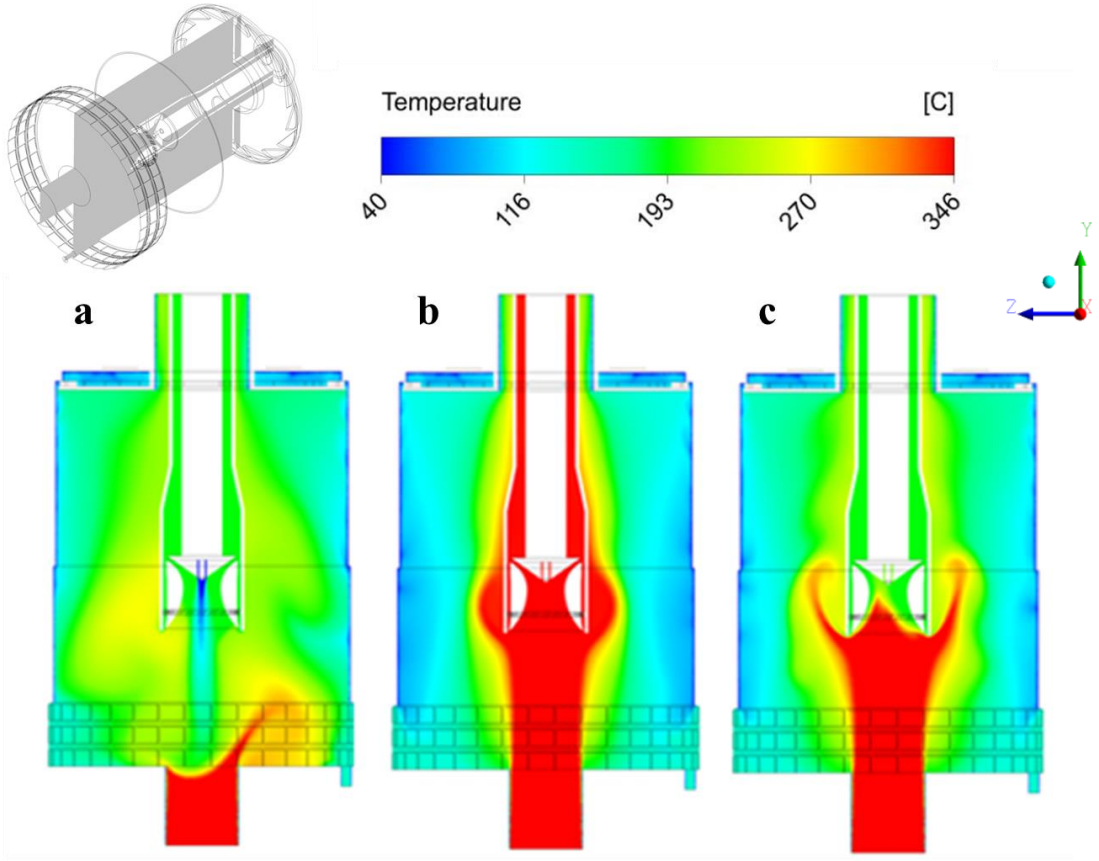

Figure 4 Axial cross-section plane of temperature patterns a) with nozzle co-flows b) without nozzle co-flows c) without cold non-rotating co- flow

stationary flow behaviour, the transition between the central hot and peripheral cold zone is not clearly distinguishable. This could be problematic for droplets that are already dried and could lead to overheating and product degradation. Further, high temperatures could lead to stickiness and wall depositions on the cylinder walls of RMD.

It can be seen that in case b), when the co-flows around the nozzle are not present, the central hot air jet is symmetric and no radial oscillations were observed during the transient solution. The hot jet is concentrated along the axis of symmetry with a gradual transition to the cold zone.

In case c), when only the rotating hot-co flow around the nozzle is applied, the hot central jet penetrates into the protective sleeve since, the non-rotating cold flow is not restricting the hot air jet. The temperature fields show an almost symmetric patterns with a slight expansion of hot and transition zone due to rotating hot co-flow that expands while the hot and cold zones are easily distinguishable. By comparing the three cases, it can be concluded that the instabilities of central hot air jet and thus the in-stationary phenomena is the result of the non-rotating cold flow.

4. Conclusions

In this study, a three-dimensional steady-state and transient CFD model of air flow in a novel RMD is developed and validated against experimental temperature measurements. The steady-state model shows good agreement with an average error of 2.5% for probes: V1 and V3 and 7.5% and 9.5% for V9 and V10 thermocouples, respectively. The results show that the desired temperature profiles with two distinct zones: central hot and a peripheral rotating cold zones can be established; however, radial oscillations of central hot air jet induced by the interaction of the hot air jet and counter nozzle co-flows can be seen. The frequency of oscillations is found to be 3.5 Hz. Further, it is found that the the instabilities arise mainly due to the cold non-rotating component of the nozzle co-flows. Such transient behaviour needs to be minimized to avoid product degradation and to have a stable and efficient spray drying operation. Future studies will aim to optimize the relative ratios of these counter-current flows and to investigate droplet drying behaviour.

5. Acknowledgements

This research is conducted within TKI-RMZD project in collaboration with Institute for Sustainable Process Technology (ISPT) within Drying and Dewatering cluster, Royal FrieslandCampina, Université Catholique de Louvain and Energy Research Centre of the Netherlands (ECN). Authors would like to express their gratitude to TKI and ISPT for the financial support and to all project members for the fruitful discussions during the meetings.

6. References

ANSYS. (2004). Fluent Manual. ANSYS. Retrieved from www.fluent.com

Broqueville, A. de, De Wilde, J., & Tourneur, T. (2018). *WO/2018/203745*. The Netherlands: V.O. Patents & Trademarks. Retrieved from https://patentscope.wipo.int/search/en/detail.jsf?docId=WO2018203745

De Wilde, J. (2014). Gas-solid fluidized beds in vortex chambers. *Chemical Engineering and Processing: Process Intensification*, *85*, 256–290. https://doi.org/02552701

De Wilde, J., & de Broqueville, A. (2008). Experimental investigation of a rotating fluidized bed in a static geometry. *Powder Technology*, *183*(3), 426–435. https://doi.org/00325910

Fletcher, D. (2017). *Computational Fluid Dynamics Simulation of Spray Dryers—An Engineer's Guide*. *CRC Press: Boca Raton* (Vol. 35). FL: Taylor & Francis. https://doi.org/0737-3937

Kieviet, F. G. (1997). *Modelling Quality in Spray Drying*. *Eindhoven University of Technology*. Eindhoven University of Technology. Retrieved from

Kuriakose, R., & Anandharamakrishnan, C. (2010). Computational fluid dynamics (CFD) applications in spray drying of food products. *Trends in Food Science and Technology*, *21*(8), 383–398. https://doi.org/09242244

Langrish, T. A. G., & Fletcher, D. F. (2003). Prospects for the modelling and design of spray dryers in the 21st century. *Drying Technology*, *21*(2), 197–215. https://doi.org/07373937

Masters, K. (1985). *Spray drying handbook*. London, UK: George Godwin Ltd.

Rahman, U. J. U., Baiazitov, I., Pozarlik, A. K., & Brem, G. (2018). CFD study of air flow patterns and droplet trajectories in a vortex chamber spray dryer. In *21st International Drying Symposium*. Valencia.

Saleh, S., & Nahi Saleh, S. (2011). Transient simulation of air flow in a co-current spray dryer. In *Euro Drying 2015* (pp. 26–28). Retrieved from https://www.researchgate.net/publication/270506995

Tourneur, T., Broqueville, A. de, & De Wilde, J. (2018). Experimental and CFD study of multi-zone vortex chamber spray dryers. In *International Symposium on Chemical Reactor Engineering-ISCRE 25*.

Wai Woo, M., Daud, W. R. W., Mujumdar, A. S., Zhonghua, W., Zainal Meor Talib, M., & Tasirin, S. M. (2009). Non-Swirling Steady and Transient Flow Simulations in Short-Form Spray Dryers. *Chemical Product and Process*

Modeling, *4*(1), 20.
Weber, J. M., Stehle, R. C., Breault, R. W., & De Wilde, J. (2017). Experimental study of the application of rotating fluidized beds to particle separation. *Powder Technology*, *316*, 123–130. https://doi.org/1873328X